Appl Nanosci (2014) 4:643–648
DOI 10.1007/s13204-013-0240-y

ORIGINAL ARTICLE

Physical properties of α-Fe_2O_3 nanoparticles fabricated by modified hydrolysis technique

Muhammad Waseem · Sajida Munsif · Umer Rashid · Imad-ud-Din

Received: 9 May 2013 / Accepted: 23 May 2013 / Published online: 7 June 2013

Abstract We have tested modified hydrolysis method for the preparation of α-Fe_2O_3 nanoparticles. The particles after synthesis were applied for a series of physicochemical techniques. Iron chloride was used as a precursor material. The particle size distribution was determined using zeta sizer and scanning electron microscopy. The surface area and the morphology of the particles vary by changing the concentration of the precursor material. The size of nanoparticles varies from 10 to 90 nm. The particles having size of 23 ± 1 nm were separated out from the solution and their size remains almost the same even after one month. Energy dispersive X-ray analysis (EDX) of Fe_2O_3 nanoparticles confirms the purity of the desired material. The weight loss of the particles with respect to the temperature was studied by thermogravimetric and differential thermogravimetric (TG/DTG) analysis. X-ray diffraction (XRD) has been employed to study the crystallinity of the particles.

Keywords Characterization · DLS studies · Hydrolysis method · Iron oxide nanoparticles

Introduction

Nanoparticles are considered to be of great scientific interest as they are considered a bridge between bulk and atomic levels. The properties of particles change as their size approaches the nanoscale which in turn provides a large surface area. A variety of nanoparticles like SiO_2, Cu, TiO_2, ZrO_2, $BaTiO_3$, $BaZrO_3$, $LiNbO_3$ and Fe_2O_3 are reported in literature (Finnie et al. 2007; Qui et al. 1999; Li and Wang 1999; Sundaram et al. 2007; Niederberger et al. 2004; Kang et al. 1996). The two main types of the oxides of iron, i.e., magnetite Fe_3O_4 and maghemite Fe_2O_3 are considered to be of great interest due to their paramagnetic properties and thus are used in many fields. Nanoparticles may or may not possess size-related properties which differentiate them from those of fine particles or bulk materials (Niederberger et al. 2004; Kang et al. 1996).

Iron oxide nanoparticles having extensive applications are the current global demand. These particles have potential applications and are used as catalytic materials, adsorbents, pigments, flocculants, coatings, gas sensors and ion exchangers. They are also used in magnetic recording devices, in toners as well as in inks for xerography. Nanosized maghemite has excellent magnetic properties and is used for biomedical purposes. These particles have been widely researched for magnetic resonance imaging (MRI), which are becoming tools for brain tumor imaging and treatment (Lodhia et al. 2010; Hadjipanayis et al. 2010). Further, these particles are also used in transparent paints, in catalysis and in numerous synthesis processes (Mohapatra and Anand 2010). In literature, iron oxide has been prepared by applying various techniques like microemulsion, precipitation, sol–gel, coprecipitation and hydrolysis methods (Lodhia et al. 2010; Hadjipanayis et al. 2010; Mohapatra and Anand 2010).

Shavel et al. (2007) prepared iron nanocrystals by treating iron oleate complex, sodium oleate and oleic acid in squalene solvent. It was found that the use of squalene as a solvent results in the formation of magnetic core/shell

M. Waseem (✉)
Department of Physics, Comsats Institute of Information Technology, Islamabad 44000, Pakistan
e-mail: waseem_atd@yahoo.com

S. Munsif · U. Rashid · Imad-ud-Din
Department of Chemistry, Hazara University, Mansehra, Pakistan

particles with cubic shape. However, Sayyad et al. (2012) synthesized iron nanoparticles from naturally occurring hemoglobin and myoglobin and found the particles to be crystalline and that their size distribution falls in the range of 2–5 nm. The effect of pH on the particle size was noted by Lodhia et al. (2010) while preparing the magnetic Fe_2O_3 nanoparticles. The particles were prepared by mixing the ferrous and ferric salts in an aqueous solution. Nidhin et al. (2008) synthesized iron oxide nanoparticles by interacting of polysaccharide templates and iron (II) sulfate in aqueous phase. They reported the crystallite size of the particles in the range of 30–35 nm. Sreeja and Joy (2007) prepared iron oxide nanoparticles using iron (II) chloride and iron (II) sulfate and the resulting crystals were found in the range 8–13 nm with an average particle size of 10 nm. Further, Katsuki and Komarneni (2001) studied the effects of temperature on the synthesis of Fe_2O_3 nanoparticles. It was found that increase in the temperature of the reactants results in the increase in particle size of the final material.

The present work thus focused on the synthesis and characterization of Fe_2O_3 nanoparticles by modified hydrolysis methods. To explore the physical properties, various analytical techniques like surface charge properties, surface area measurements, dynamic light scattering (DLS) studies, scanning electron microscopy (SEM), energy dispersive X-rays (EDX) analysis, X-ray diffraction (XRD) and thermogravimetric and differential thermogravimetric (TG/DTG) analyses were employed to the final material.

Experimental

Reagents

Analytical grade reagents were used without any further purification. $FeCl_3{\cdot}6H_2O$ and NaCl were supplied by Merck while NaOH was provided by BDH chemicals. All the solutions were prepared in double distilled water. The pH of the solutions was carefully adjusted with the required amount of HCl and NaOH solution.

Preparation of α-Fe_2O_3 nanoparticles by modified hydrolysis technique

α-Fe_2O_3 nanoparticles were prepared by the drop-wise mixing of 3.33 ml of $FeCl_3{\cdot}6H_2O$ (3 M) solution with 9.99 ml of HCl (0.234 M) solution. After complete mixing, the contents were diluted to 1 L with double distilled water and the concentration of Fe^{3+} was achieved to be 0.01 M/L. The iron hydroxide was first formed which was then aged for 48 h. After aging, the suspension was preserved at 96 °C for 48 h in silicon oil bath. The contents were agitated with constant stirring speed of 200 rpm. The mixture was finally quenched in cold water and the orange red color that appeared confirmed the formation of α-Fe_2O_3 nanoparticles. Afterward, the solution was dried in an oven at 100 °C. Finally, the fine powder of α-Fe_2O_3 nanoparticles was stored in polyethylene vessels. Similarly α-Fe_2O_3 nanoparticles were also synthesized by reacting dilute solutions of iron chloride with HCl. 99 mM $FeCl_3.6H_2O$ solution was mixed drop-wise with 6.6 mM solution of HCl. The contents were preserved at 96 °C for 48 h. The rest of procedure was the same as adopted for the preparation of the nanoparticles by reacting the concentrated solutions.

Characterization of α-Fe_2O_3 nanoparticles

After the synthesis of iron oxide nanoparticles, the powder samples were analyzed by various analytical techniques like surface area measurements, SEM/EDX, TG/DTA, XRD, particle size distribution and surface charge properties.

The isoelectric point (IEP) values of α-Fe_2O_3 nanoparticles were determined at different concentrations of the background electrolyte using the method described by Davis et al. (1978). NaCl having concentration 0.01 M has been selected as a background electrolyte. 0.1 g of Fe_2O_3 nanoparticles was dispersed in the electrolytic solution. The suspension was adjusted to pH 2 which was equilibrated for 20 min. The pH of the suspension was measured by pH meter model Mettler Toledo MP 220. After pH equilibration, 0.3 ml of 0.1 M NaOH was added from the burette to the solution having Fe_2O_3 nanoparticles. The suspension was stirred at 120 rpm and the pH of the solution was noted after 2 min. This process continued till the final pH of the suspension approached 11. Similar experiments were performed by taking 0.1 and 1 M solution of NaCl as background electrolyte. The mean charge on the surface of the particles was determined by plotting Q vs. pH of the suspension.

The BET surface area, pore volume (V_P) and average pore diameter (D_{BJH}) of the iron oxide nanoparticles are determined by nitrogen adsorption method at 77 K using surface area analyzer model Quantachrome Nova 1200e. The sample after degassing at 105 °C for 1 h was subjected for surface area measurements. The particle size distribution is measured using particle size analyzer model Malvern Nano-ZS90 (UK). Before analysis, 0.01 mg of the solid is added to the flask having 40 ml of aqueous solution. To avoid agglomeration, the suspension was sonicated for 30 min. After that, a small aliquot of the suspension was taken in the Laser Doppler Velocimeter and was analyzed for size distribution. The Rayleigh-Debye model was used for the distribution function analysis (Hiemanz

and Rajagopalan 1997). The morphology of iron oxide nanoparticles were determined by scanning electron microscopy. The micrographs of the sample were obtained in SEM model JSM 5910 (JEOL Co Japan) at 20 keV. The elemental percentage present in the solid was determined in micro analyzer model INCA 200 (UK). Before analysis, the nanoparticles were deposited on to a double stick tape fixed to an aluminum sample holder and were sputter-coated with gold in sputter coater model SPI-MODULE (USA) for 90 s at 30 mA. To find the crystallinity, X-ray diffraction pattern of the dried sample was recorded by using JEOL XRD, model JDX-3532 with Mn filtered Cu-Kα radiations. X-ray diffraction pattern was taken by measuring 2θ values from 10° to 80° with a step size of 0.30° and step time of 5 s. The operating voltage and current are 40 kV and 20 mA, respectively. TGA is a technique in which the weight of the sample was measured as a function of temperature, under controlled heating. TG and DTG analyses of iron oxide nanoparticles were recorded in TG/DTA model Perkin Elmer model 6300. The known weight of the sample was heated up to 1,000 °C with a heating rate of 10 °C/min under air atmosphere.

Results and discussion

Characterization of nanoparticles

The physiochemical characteristics of the iron oxide nanoparticles used in the present investigation and the techniques employed are given below.

Surface area and charge properties of α-Fe_2O_3 nanoparticles

The specific Brunauer Emmett and Teller (BET) surface area and pore size information of the solids were collected by N_2 adsorption method. The BET surface area for iron oxide nanoparticles prepared by concentrated solutions was found to be 90.71 m^2/g and from the same method, where the dilute solutions were used, the surface area was found to be 93.84 m^2/g. Similarly, the pore volume and pore diameter for the particles prepared using concentrated solution are found to be 0.61 cc/g and 10.8 nm, respectively, whereas these values for the particles synthesized using dilute solution were 0.85 cc/g and 12.9 nm. These results show that by decreasing the concentration of reacting species the particles formed will display high surface area. Further, by selecting the dilute concentrations, the pore volume and pore diameter were improved.

The potentiometric titration plots for the particles at room temperature and in different electrolytic concentrations are depicted in the Fig. 1. This figure showed that the

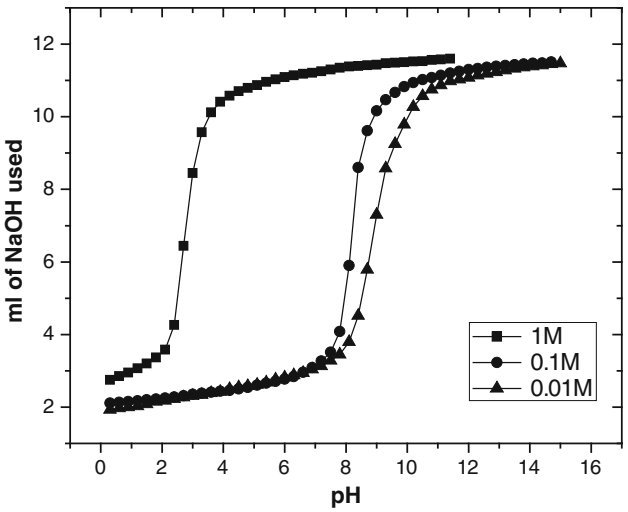

Fig. 1 pH vs. ml of NaOH used for α-Fe_2O_3 nano particles

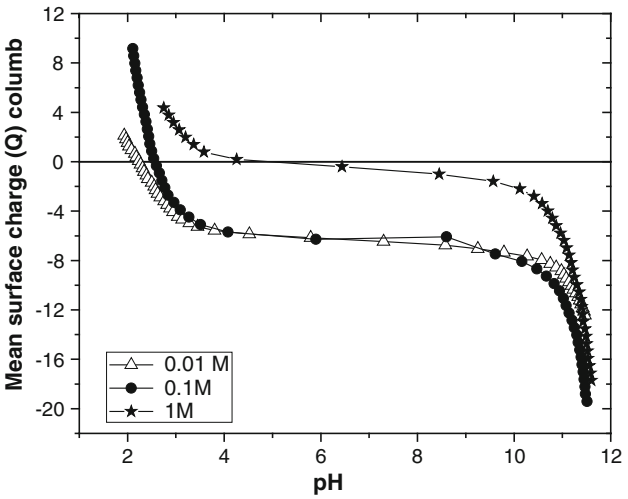

Fig. 2 Mean surface charge of α-Fe_2O_3 nano particles by potentiometric titration method

concentration of background electrolyte has a marked effect on shifting the potentiometric titration curve. The curves further show that more OH^- ions were required to neutralize H^+ ions when the concentration of NaCl was decreased from 1 to 0.01 M. Therefore, more volume of the base was used up while decreasing the concentration of the background electrolyte. The potentiometric titration curves for 0.1 and 0.01 M show that Na^+ ions play a role in the neutralization of OH^- ions along with H^+ ions where a slow increase in the pH was observed till the pH value of 7.8. However, an increased effect for 1 M electrolytic solution was noted where a sudden jump in the pH value was observed. This behavior shows that the surface became more negative when the pH was increased from 2.3. The curves for the mean surface charge vs. pH of the solution were shown in the Fig. 2. It can be seen from this figure that in the charging mechanism of the Fe_2O_3 nanoparticles

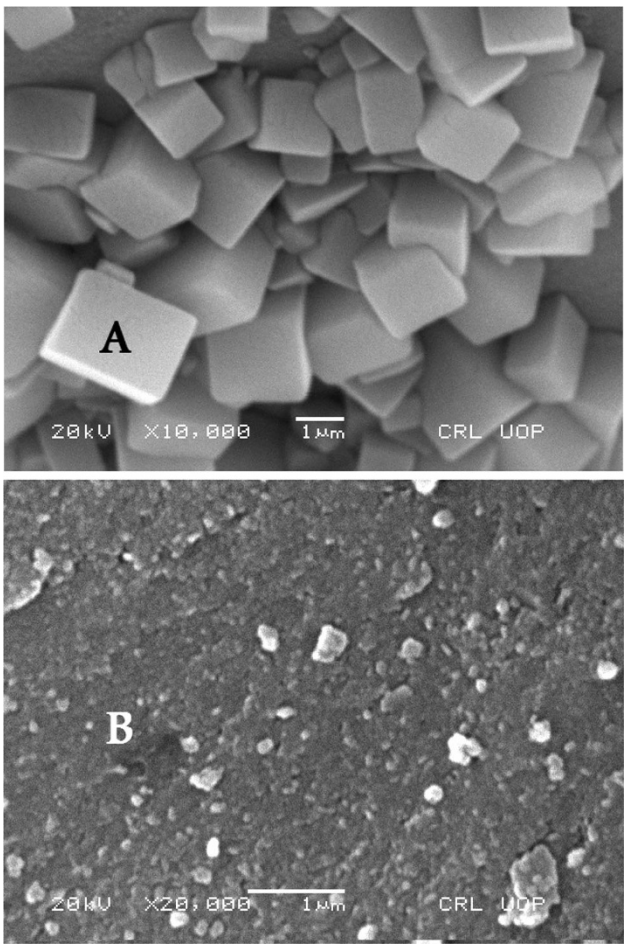

Fig. 3 SEM micrograph of α-Fe_2O_3 nano particles using **a** concentrated and **b** dilute solution synthesized by hydrolysis method

the effect of sodium (Na^+) ions is greater than the corresponding effect of chloride (Cl^{-1}) ions. It shows that shielding effect of the Cl^{-1} ions increases as its concentration rises. These curves also show that the IEP values of α-Fe_2O_3 nanoparticles increases with an increase in the concentration of the background electrolyte. Thus, increase in the ionic strength of the background electrolyte shifts the IEP to the basic region, indicating a higher association affinity for negative ions compared with positive ions. The IEP value was found to increase from 2.2 to 2.7 and 4.1 by increasing the concentration of NaCl from 0.01 to 0.1 and 1 M, respectively. Thus it is concluded that IEP increases with the increase in the molar concentration of NaCl solution. This increase in the IEP is usually expected for the hydrophilic substances where the OH^- groups from the base can react with the metal cation of electrolyte which has already been sorbed on the surface of the solid particles. In present case, at low pH values of 2.2–4.2, the hydroxyl ions seem to interact with the Na^+ ions resulting in the slow release of protons from the nano particles. However, the release of Na^+ ions was not appreciable when the pH of the suspension increased from 4.4 to 9. In this pH range deprotonation has taken place with bit faster rate. Thus the role of Cl^- ions may be effective in shifting the IEP towards the higher pH value by charging the surface of the particles negatively.

Scanning electron microscopy (SEM) and energy dispersive X-ray (EDX) analysis

The surface morphology of iron oxide nanoparticles was investigated by SEM and EDX analyses. The SEM micrographs of iron oxide nanoparticles are shown in Fig. 3. The micrograph obtained for the concentrated solution show that the particles were not of same sizes. However, they are visible and clearly seen as cubic crystals with the size varying from 500 nm to 2 μm. The micrograph obtained for the particles prepared by dilution method shows that the nanoparticles were irregular in size and shape and vary from 10 to 90 nm with aggregation. EDX analysis reported in Fig. 4 showed that the respective percent weight of oxygen and iron on the surface of iron oxide nanoparticles was found to be 22.07 and 77.93 %. The EDX data displayed only the peaks for Fe and O atoms which thus confirmed the absence of any impurities during the preparation of desired material.

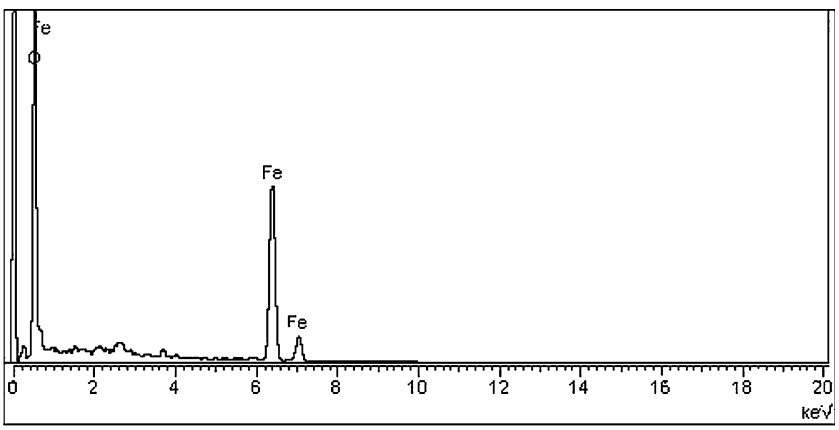

Fig. 4 EDX analysis of α-Fe_2O_3 nanoparticles synthesized by hydrolysis technique

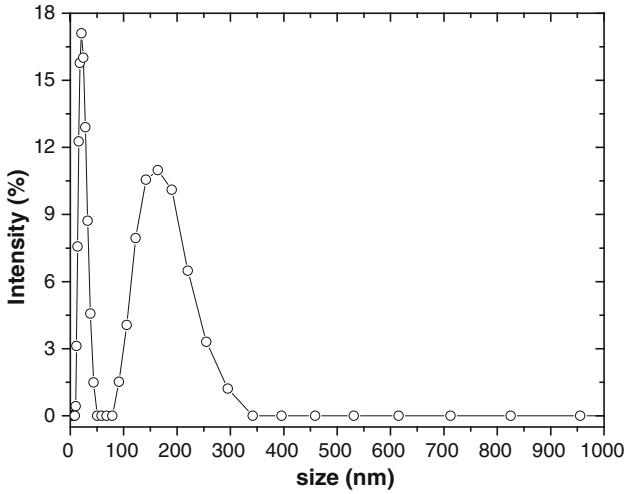

Fig. 5 DLS studies of α-Fe_2O_3 nanoparticles

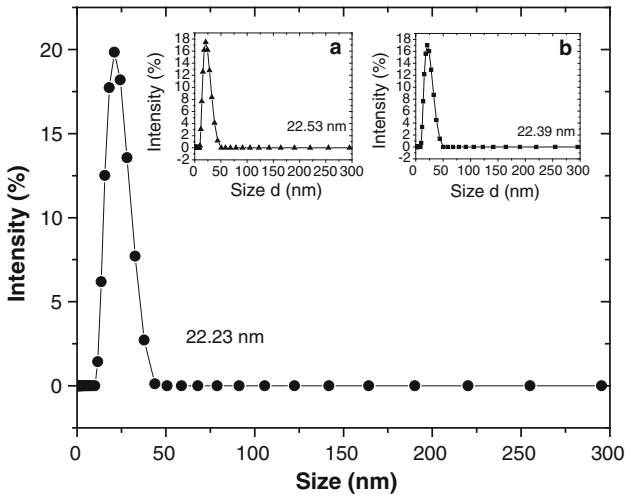

Fig. 6 Size studies of α-Fe_2O_3 nanoparticles. *Inset a* analysis after 15 days *b* analysis after 30 days

Particle size distribution

The Rayleigh-Debye model was used for the distribution function analysis of suspension system. The particle size distribution curves for α-Fe_2O_3 nanoparticles are shown in Figs. 5 and 6. The dynamic light scattering (DLS) data for Fe_2O_3 displayed two peaks (Fig. 5) having the diameter of 23 and 178 nm. The average particle size was found to be 85 nm, showing that all the particles were not of same size. The increase in the mean particle size can also be attributed to the agglomeration of smaller particles. The nanoparticles having size 23 nm were separated by using nano sieves. Inset of Fig. 6a shows that the particles were found stable after 15 days of DLS test, while inset of Fig. 6b points the stability of nanoparticles even after 30 days.

XRD and TG/DTG analyses

XRD was employed to detect the phase of the nanoparticles. All peaks of the XRD patterns were matched with the phase of α-Fe_2O_3 (JCPDS No. 33-0664) containing hkl planes at (220), (104), (110) and (024). The highest peak appeared at 33° which is an indication of the presence of α-Fe_2O_3 (Zhao et al. 2007). Figure 7 represents thermo gravimetric and differential thermo gravimetric analyses. Three stages of weight loss were observed. The total weight loss recorded was 1.633 mg of the weight taken. The sudden weight loss of 0.436 mg and a gradual weight loss of 0.681 mg may be assigned to the superficial water loss, while a weight loss of 0.516 mg can be associated with the loss of chemisorbed water. The DTG curve also demonstrates the loss of water losses from the surface as well water bonded in the interstices of the solid network. Two distinct peaks were observed at the temperature of 78 and 280 °C, respectively, associated with the removal of

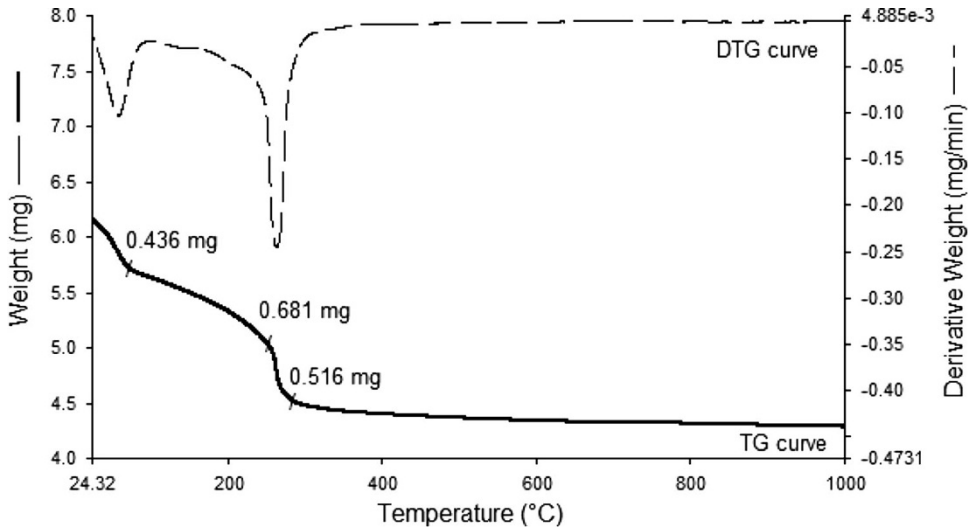

Fig. 7 TG and DTG analyses of α-Fe_2O_3 nanoparticles

surface and interstitial waters. The DTG curve supports the data collected from TG measurements.

Conclusion

From the above discussion it can be concluded that the hydrolysis method is suitable for the successfully synthesizing Fe_2O_3 nanoparticles. The DLS technique confirms that the size of the nanoparticles was around 23 nm. These particles were found stable even for 30 days and no agglomeration was detected. The respective BET surface area for iron oxide nanoparticles prepared in concentrated and dilute solutions of the precursor material was found to be 90.71 and 93.84 m^2/g. These results show that nanoparticles with high surface area can be prepared by decreasing the concentration of reacting species. The EDX spectroscopy confirms the purity of the particles. The background electrolyte concentration of the system has a profound effect on the titration curves and with increase in concentration of background electrolyte, a shift towards higher pH value is observed, i.e., the IEP of Fe_2O_3 nanoparticles is found to increase with the concentration of the background electrolyte. The alpha phase of the nanoparticles has been detected by applying XRD. The weight losses obtained from TG data were associated with the removal of adsorbed and bonded water.

Acknowledgments We gratefully acknowledge Higher Education Commission (HEC) of Pakistan for supporting this work under project No: PM-IPFP/HRD/HEC/2012/2729.

References

Davis JA, James RO, Leckie JO (1978) Surface ionization and complexation at the oxide/water interface. I. Computation of electrical double layer properties in simple electrolytes. J Colloid Interface Sci 63:480–499

Finnie KS, Bertlett JR, Barbe CJA, Kong L (2007) Formation of silica nanoparticles in microemulsions. Langmuir 23:3017–3024

Hadjipanayis CG, Machaidze R, Kaluzova M, Wang L, Schuette AJ, Chen H, Mao X, Wu H (2010) EGFRvIII antibody-conjugated iron oxide nanoparticles for magnetic resonance imaging-guided convection-enhanced delivery and targeted therapy of glioblastoma. Cancer Res 70:6303–6312

Hiemanz PC, Rajagopalan R (1997) Principles of colloids and surface chemistry. Marcel Dekker Inc, New York 193

Kang YS, Risbud S, Rabolt JF, Stroeve P (1996) Synthesis and characterization of nanometer-size Fe_3O_4 and γ-Fe_2O_3 Particles. Chem Mater 8:2209–2211

Katsuki H, Komarneni S (2001) Microwave-hydrothermal synthesis of monodispersed nanophase α-Fe_2O_3. J Am Ceram Soc 84: 2313–2317

Li GL, Wang GH (1999) Synthesis of nanometer-sized TiO_2 particles by a microemulsion method. Nanostruct Mater 11:663–668

Lodhia J, Mandarano G, Ferris NJ, Eu P, Cowell SF (2010) Development and use of iron oxide nanoparticles (Part 1): synthesis of iron oxide nanoparticles for MRI. Biomed Imaging Interv J 6:e12

Mohapatra M, Anand S (2010) Synthesis and applications of nanostructured iron oxides/hydroxides–a review. Inter J Eng Sci Technol 2:127–146

Nidhin M, Indumathy R, Sreeram KJ, Nair BU (2008) Synthesis of iron oxide nanoparticles of narrow size distribution on polysaccharide templates. Bull Mater Sci 31:93–96

Niederberger M, Pinna N, Polleux J, Antonietti M (2004) A general soft-chemistry route to perovskites and related materials: synthesis of $BaTiO_3$, $BaZrO_3$, and $LiNbO_3$ nanoparticles. Angew Chem 43:2270–2273

Qui S, Dong J, Chen G (1999) Preparation of Cu nanoparticles from water-in-oil microemulsions. J Colloid Interface Sci 216:230–234

Sayyad AS, Balakrishnan K, Ci L, Kabbani AT, Vajtai R, Ajayan PM (2012) Synthesis of iron nanoparticles from hemoglobin and myoglobin. Nanotech 23:055602

Shavel A, Rodriguez-Gonzalez B, Spasova M, Farle M, Liz-Marzan LM (2007) Synthesis and characterization of iron/iron oxide core/shell nanocubes. Adv Funct Mater 17:3870–3876

Sreeja V, Joy PA (2007) Microwave-hydrothermal synthesis of γ-Fe_2O_3 nanoparticles and their magnetic properties. Mater Res Bull 42:1570–1576

Sundaram NTK, Vasudevan T, Subramania A (2007) Synthesis of ZrO/sub2/nanoparticles in microwave hydrolysis of Zr (IV) salt solutions-Ionic conductivity of PVdF-co-HFP-based polymer electrolyte by the inclusion of ZrO/sub2/nanoparticles. J Phy Chem 68:264–271

Zhao B, Wang Y, Guo H, Wang J, He Y, Jiao Z, Wu M (2007) Iron oxide(III) nanoparticles fabricated by electron beam irradiation method. Mater Sci Poland 25:1143–1148